CORA Cork Open Research Archive
Cartlann Taighde Oscailte Chorcaí

Title	Performance characterization of a battery-less NFC sensor for museum artifact monitoring
Authors	Gawade, Dinesh R.;Kumar, Sanjeev;Simorangkir, Roy B. V. B.;O'Callaghan, Brendan;Iacopino, Daniela;Rather, Nadeem;O'Flynn, Brendan;Buckley, John L.
Publication date	2023-07-03
Original Citation	Gawade, D. R., Kumar, S., Simorangkir, R. B. V. B., O'Callaghan, B., Iacopino, D., Rather, N., O'Flynn, B. and Buckley, J. L. (2023) 'Performance characterization of a battery-less NFC sensor for museum artifact monitoring', 2023 34th Irish Signals and Systems Conference (ISSC), Dublin, Ireland, pp. 1-7. doi: 10.1109/ISSC59246.2023.10162126
Type of publication	Conference item
Link to publisher's version	10.1109/issc59246.2023.10162126
Rights	© 2022, IEEE. Personal use of this material is permitted. Permission from IEEE must be obtained for all other uses, in any current or future media, including reprinting/republishing this material for advertising or promotional purposes, creating new collective works, for resale or redistribution to servers or lists, or reuse of any copyrighted component of this work in other works.
Download date	2026-11-07 02:49:58
Item downloaded from	https://hdl.handle.net/10468/14714

UCC
University College Cork, Ireland
Coláiste na hOllscoile Corcaigh

Performance Characterization of a Battery-less NFC Sensor for Museum Artifact Monitoring

Dinesh R. Gawade†, Sanjeev Kumar†, Roy B. V. B. Simorangkir†, Brendan O'Callaghan§, Daniela Iacopino†, Nadeem Rather†, Brendan O'Flynn†, John L. Buckley†,
†Tyndall National Institute, University College Cork, Dyke Parade, T12R5CP, Cork, Ireland.
§Microelectronic Circuits Centre Ireland (MCCI), Tyndall National Institute, Dyke Parade, T12R5CP, Cork, Ireland.
E-mail: dinesh.gawade@tyndall.ie

***Abstract*—This paper presents the performance of a battery-less near field communication (NFC) sensor for museum artifact monitoring. The radio frequency (RF) receiver sensitivity of the NFC sensor was measured using a commercial Tagformance measurement system. To respond to read commands, the NFC sensor requires a minimum magnetic field strength of 67.8 mA/m in free space, and 87.6 mA/m after integration within an archive box typically used for cultural heritage artifact storage. The integrated NFC loop antenna has a -3 dB bandwidth of 1.16 MHz in free space and 1.14 MHz bandwidth when integrated within the archive box. These measured RF sensitivity and -3 dB bandwidth values are in close agreement with the ISO/IEC 15693 standard. This work demonstrates a DC power consumption of 597 μW which is shown to be the lowest value compared to the state-of-the-art literature. In addition, the wireless communication range of approximately 5 cm was achieved which compares favourably with the maximum read ranges reported in literature. The developed NFC sensor has been deployed in European museums for wireless monitoring of valuable artifacts.**

***Index Terms*—battery-less NFC sensor, cultural heritage objects, energy harvesting; HF-RFID, museum artifacts monitoring, NFC sensor characterization, Voyantic Tagformance.**

I. Introduction

Museum artifacts and cultural heritage objects are prone to rapid deterioration due to exposure to unstable climatic conditions and environmental pollutants. This is particularly true for historic papers and documents containing iron gall ink, which are vulnerable to damage from even small fluctuations in temperature and humidity [1]. However, many valuable artifacts and documents are stored in museum buildings without proper climate control mainly because modern air conditioning and Heating, ventilation, and air conditioning (HVAC) systems are complex and expensive to implement. Therefore, monitoring the microclimatic conditions in a museum is crucial for preventive conservation, even in areas with climate control [1]–[4]. For instance, real-time monitoring of temperature and humidity can help museum owners prevent artifact degradation caused by factors such as shrinkage or mold growth.

Due to the increasing number of Internet of Things (IoT) applications, the last few years have witnessed a significant advancement in the development of battery-less wireless sensing devices [5], [6] and many of these IoT applications (e.g., museum artifacts monitoring) require low or no maintenance cost [7]. In addition, the advancement in low to ultra-low power electronics systems [7] and sensors has steered the rapid growth of battery-less wireless sensing devices, particularly those based on radio-frequency identification (RFID) and near field communication (NFC) technologies [8]. In recent years, the market for NFC technology has increased significantly due to the incorporation of NFC reader capability within smartphones [9]. Currently, NFC technology not only enables contact-less payments, but also enables passive wireless measurement of multiple parameters, including soil moisture [10], [11], fruit quality [12], [13], long-term building structural health monitoring [14], gas monitoring [15], cattle health parameter monitoring [16] and environmental parameter monitoring [10], [17], to name a few.

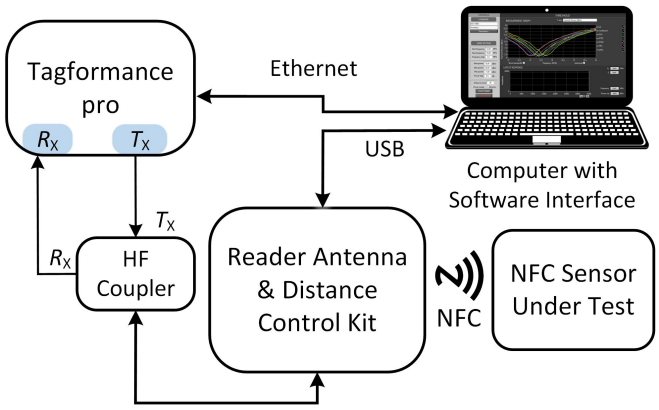


Fig. 1. Block diagram of the NFC sensor characterization setup.

However, only a few research articles have reported on the characterization of key parameters of NFC sensor transponders, such as radio frequency (RF) receiver sensitivity, -3 dB bandwidth, quality factor (Q), as well as wireless communication performance of the sensor [18]–[21]. Effective analysis and optimization of such key performance parameters is crucial for battery-less sensing applications, for instance, monitoring of health related parameters [22] and museum artifacts [23].

This paper presents the performance characterization of a battery-less NFC sensor transponder using an an industry standard Tagformance Pro measurement system from Voyantic Ltd, Finland [24]. The key measurement parameters include RF receiver sensitivity (i.e., the RF power required for the NFC sensor to be able to respond to the command), DC power consumption and wireless communication range.

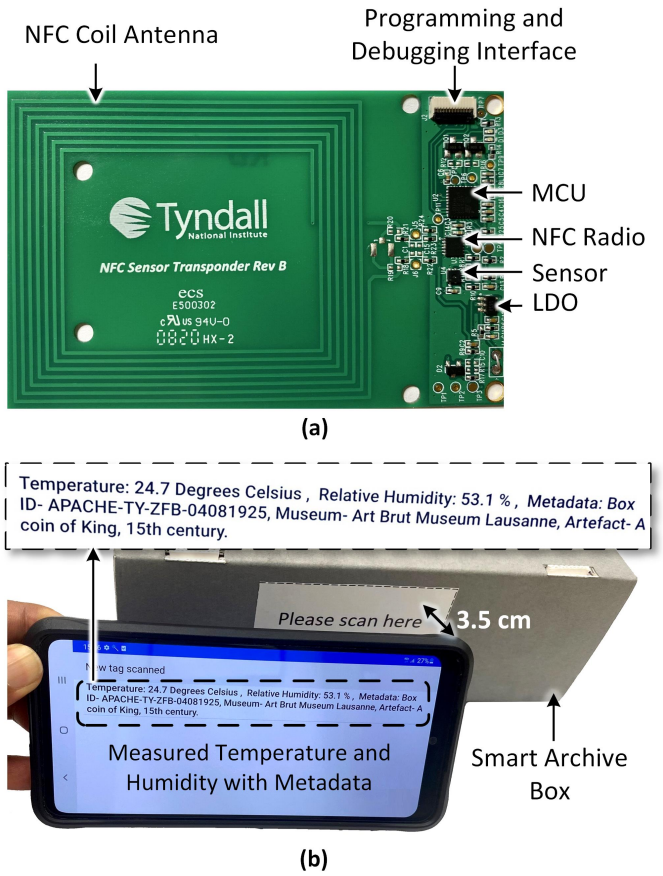


Fig. 2. Battery-less NFC sensor and smart archive box [26].

Fig. 1 shows the block diagram of the NFC sensor characterization setup, which includes Tagformance Pro, NFC reader Antenna (Part Number: C145), distance control kit and a computer with an appropriate software interface, i.e., Tagformance HF. As reported in Tagformance's technical manual [25], the NFC reader (C145) sends commands to the sensor transponder by modulating the carrier signal. The transponder then reflects the signal back by using load modulation. To assess the NFC sensor's performance, dedicated commands such as Inventory and Read Single Block defined by ISO/IEC 14443 and ISO/IEC 15693 standards are used. The Tagformance tool sends these commands and acts as a time-domain network analyzer while providing a carrier signal for the transponder and recording its response. The software interface on a computer is used to visualize the measured parameters as shown in Fig. 1.

The paper is structured as follows: Section II briefly describes the developed NFC sensor and the smart archive box which was utilized for characterization. The results of the NFC sensor measurements are presented in Section III and discussed in Section IV. Finally, Section V concludes the paper by summarizing the key findings of this work.

II. Battery-less NFC Sensor Transponder and Smart Archive Box

In previous work [26], the authors have reported on a smart museum archive box that featured a fully integrated wireless-powered temperature and humidity sensor. This sensor was designed to monitor historical, valuable, and paper-based cultural heritage objects. Fig. 2(a) shows the hardware prototype of the developed solution, which is implemented in a PCB configuration with dimensions of 85.60 mm × 53.90 mm. The inductive NFC coil antenna is designed with 7 turns, a trace width (T_{W}) of 0.6 mm, a turn spacing (T_{S}) of 0.75 mm, and a copper thickness (t_{CU}) of 35 μm. This results in a measured inductance of 6.5 μH at 13.56 MHz [26]. The NFC radio transceiver has an integrated capacitance that connects to the loop antenna to create a parallel LC circuit. This circuit has a resonant frequency of 13.56 MHz. In addition, the Fig. 2(a) also shows the microcontroller (MCU), temperature and humidity sensor (Temp and RH), low dropout voltage regulator (LDO), and programming interface, the functionalities of which were discussed by the author in [23]. Furthermore, in previous work [23], [26], the authors reported that the total DC power consumption of electronic components, including the MCU, LDO, and temperature and humidity sensor, amounted to 11.07 mW based on the power consumption values specified in their respective datasheets. Specifically, the MCU alone accounted for 8.1 mW, which represented 73.17% of the overall power consumption of the NFC sensor. As such, the optimization of the MCU's DC power consumption is the primary focus of this study.

The design uses a 4-layer PCB stack-up with a thickness of 0.8 mm, and all the electronic components are placed on the top layer to enable a planar structure that can be easily integrated into the cardboard archive box later on as discussed in [26]. The low power consumption of the NFC sensor, i.e. 597 μW yields a wireless communication range of approximately 5 cm in free space using a Samsung Galaxy S20 smartphone, as previous reported [23], [27]. Fig. 2(b) demonstrates wireless power transfer and communication between the same smartphone and the NFC sensor that was integrated within an archive box. In this case, a wireless communication range of 3.5 cm was achieved when the NFC sensor was integrated within the archive box and the range was measured from the outside, as shown in Fig. 2(b).

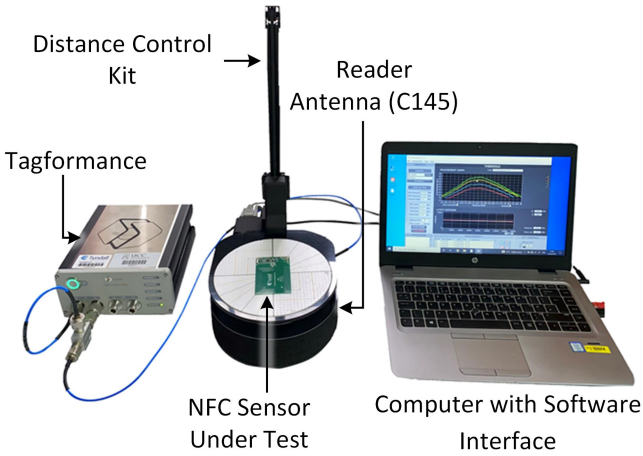


Fig. 3. NFC sensor characterization in free space using Voyantic Tagformance.

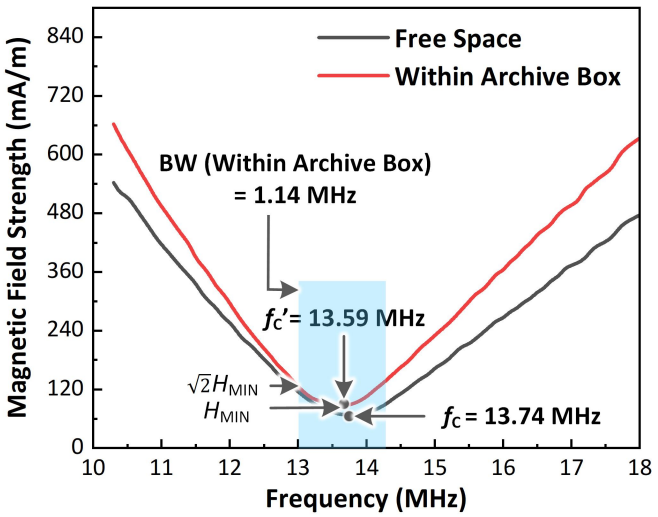


Fig. 4. Measured receiver sensitivity, -3dB bandwidth and f_C.

III. Results

This section discusses the measurement and characterization of the battery-less NFC sensor transponder in two scenarios, (a) in free-space and (b) after integration within the archive box. Fig. 3 shows the measurement setup for characterizing the performance of the sensor in free-space using a Voyantic Tagformance. Note that the same measurement setup and method were used to characterize the sensor performance for the second scenario i.e., after integrating the sensor into the archive box. The key performance parameters include RF receiver sensitivity, wireless communication range using Tagformance and NFC-enabled smartphone and DC power consumption.

A. RF Receiver Sensitivity Measurement

The RF receiver sensitivity of the NFC sensor was measured by performing a transmit power sweep from -10 dBm to + 25 dBm in the frequency range of 10 MHz to 20 MHz. In order to measure the RF sensitivity, the wireless communication distance between the reader antenna (C145) and the NFC sensor was set at 3 cm in both scenarios, i.e. NFC sensor in free space and after integration within the archive box. Fig. 4 shows the measured RF receiver sensitivity result. In free space, the NFC sensor requires a minimum magnetic field strength H_{MIN} of 67.8 mA/m at 13.74 MHz to be able to respond to the reader command from the reader and ensures the NFC sensor is readable by the reader. On the other hand, when the NFC sensor was integrated within the archive box, the NFC sensor requires a minimum magnetic field strength H_{MIN} of 87.6 mA/m at 13.59 MHz. The Tagformance software algorithm then calculates the centre frequency f_C and quality factor (Q) of the NFC sensor with the help of the measured H_{MIN}. As defined in the Tagformance technical manual [25], the threshold value of $\sqrt{2}H_{MIN}$ is used by the Tagformance software algorithm to calculate the minimum frequency f_{MIN} and maximum frequency f_{MAX}. It is evident from Fig. 4 that the calculated f_C in free space is 13.74 MHz.

TABLE I
Comparison of the NFC sensor performance parameter with ISO15693.

Parameter	Free-space	Within archive box	ISO 15693 specification
H_{MIN} (mA/m)	67.8	87.6	150 [28]
f_C (MHz)	13.74	13.59	13.56 [28]
Q at f_C	11.80	11.91	NA
−3 dB BW (MHz)	1.16	1.14	0.908 [28]

However, after integration within the archive box, the calculated centre frequency f_C' is 13.59 MHz, which is close to the required centre frequency of 13.56 MHz with a difference of 30 kHz. The centre frequency (also referred to as resonant frequency, f_R, in this case) of the NFC sensor was decreased by 0.15 MHz after integration within the archive box (f_C-f_C'). This reduction in the f_R can be described by the expression shown in Equation 1.

$$f_R = \frac{1}{2\pi\sqrt{L(C_{IC} + C_P + C_T)}} \quad (1)$$

Where, L is the inductance of the NFC loop antenna in Henrys and C_{IC} is the internal capacitance of the NFC radio in Farads. Parameter C_P is the parasitic capacitance, which mainly includes the parasitic capacitance of the loop, and C_T is the external capacitor that may be required to adjust the f_R to the operation frequency. The placement of the archive box close to the NFC sensor increases the inter-turn capacitance (C_P) of the NFC loop antenna [29]. This leads to reduction in the resonant frequency from Equation 1.

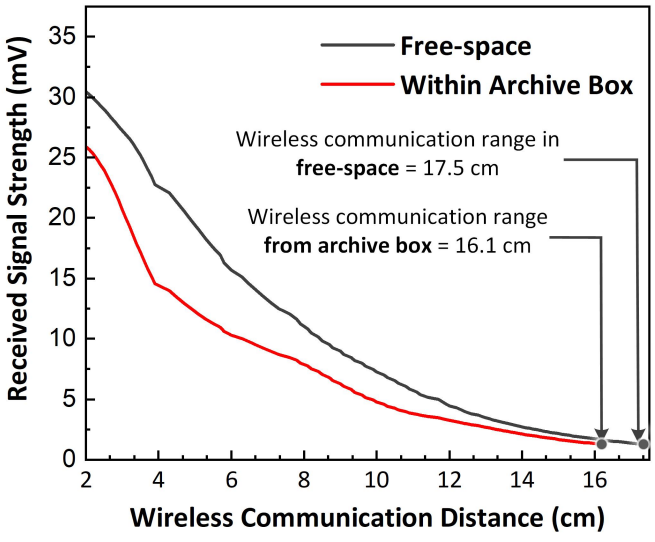


Fig. 5. Wireless communication range measurement.

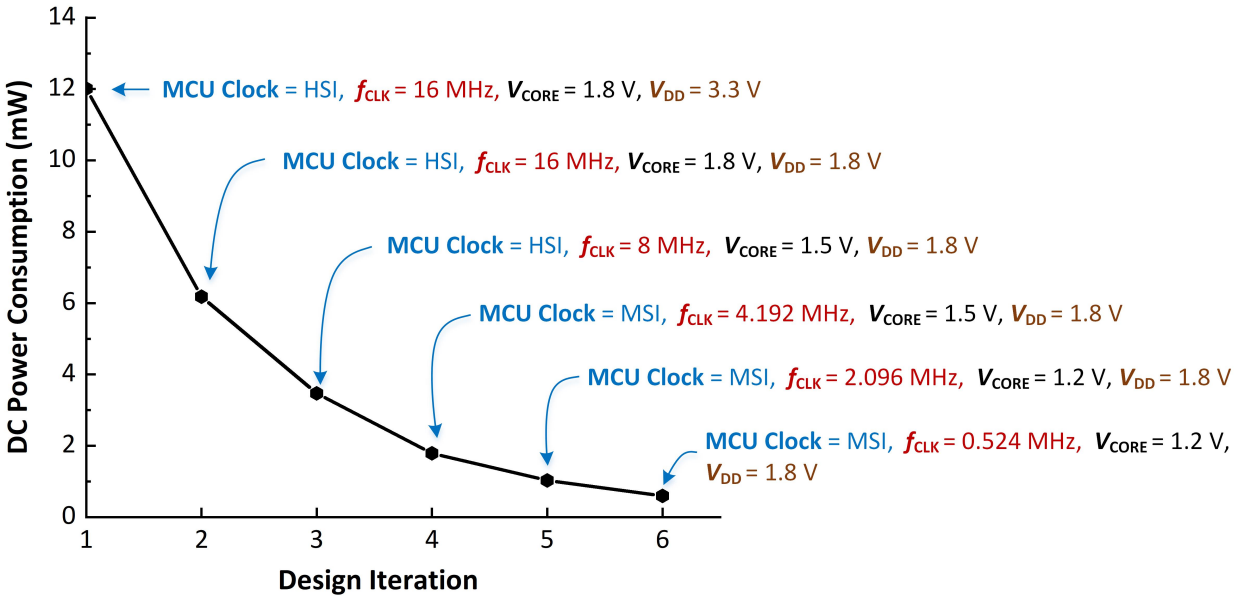


Fig. 6. Measured DC power consumption with voltage and frequency scaling

The Tagformance software algorithm uses the expression shown in Equation 2 to calculate the quality factor (Q) and -3 dB bandwidth (BW) of the NFC sensor [29], [30]. The measured and calculated performance parameters of the NFC sensor are summarized in Table I.

$$Q = \frac{f_C}{BW} = \frac{f_C}{f_{MAX} - f_{MIN}} \tag{2}$$

The comparison in Table I shows that the performance of the developed NFC sensor is in agreement with the ISO/IEC 15693 air interface and initialization specification [28].

B. Wireless Communication Range Measurement using Tagformance

As shown in Fig 3, a distance control kit within the Tagformance pro was used to automatically adjust the wireless communication range. In this measurement, the Tagformance was configured with the following parameters: (a) Wireless communication range sweep = 1 cm to 18 cm with a resolution of 0.1 cm, (b) Transmit power level = + 25 dBm, (c) Modulation Index = 100 %, (d) Command = Read single block, and (e) centre frequency f_C = 13.74 MHz for free space and 13.59 MHz for after archive archive box integration scenario. For all wireless communication range distance settings, i.e. from 1 cm to 18 cm, the received signal strength (also referred to as load modulation or load modulated signal) of the NFC sensor was recorded. In this case, the load modulation is a modulated carrier signal that is reflected or returned from the NFC sensor in response to the "read single block" command. The measured wireless communication range of the NFC sensor is a function of received signal strength as shown in Fig. 5. It is evident from Fig. 5 that a wireless communication range of approximately 17.5 cm for the free space case and 16.1 cm for the archive box integration case was achieved. Note that the above 16.1 cm range does not include the inner wall thickness of the archive box of approximately 1.5 cm.

C. Wireless Communication Range Measurement using Smartphone

The wireless communication range of the NFC sensor was also measured using a Samsung Galaxy S20 smartphone. The low power consumption of the NFC sensor i.e., 597 µW yields a wireless communication range of approximately 5 cm in free space (discussed in next subsection) [23], [27]. Using the same smartphone, a wireless communication range of 3.5 cm was achieved when the NFC sensor was integrated within the archive box and the range was measured from the outside, as shown in Fig. 2.

D. DC Power Consumption

In order to decrease the harvested DC power consumption of the developed NFC sensor, voltage and frequency scaling techniques have been employed [26], [44]. As reported in previous works [23], [26], [44], the strength of the magnetic field between two mutually-coupled coils (i.e., the Smartphone Coil and NFC sensor coil) decays proportionally to the cube of the distance between them. This implies that the available RF power harvested by the NFC sensor is limited for a given distance from the Smartphone. Therefore, the DC power consumption of the NFC sensor has been optimized for low power operation as described below. Fig. 6 summarizes the measured DC power consumption as a function of MCU voltage and clock frequency. As depicted in Fig. 6, a measured DC power consumption of 12.01 mW was observed at the first design iteration with the following clock and voltage settings: Supply voltage (V_{DD}) = 3.3 V, MCU core voltage (V_{CORE}) = 1.8 V, MCU clock source = high speed internal (HSI) RC oscillator, CPU clock (f_{CLK}) = 16 MHz and I2C core input clock (f_{I2C}) = 16 MHz.

TABLE II
COMPARISON OF WIRELESS TECHNOLOGY TECHNICAL PARAMETERS.

A	B	C	D	E	F	G	H
Ref.	**RFID air interface**	**Integrated processing unit**	**MCU clock (MHz)**	**Tag Coil size (mm)**	**DC Power consumption (mW)**	**Range (cm)**	**Sensing parameters**
[9]	ISO14443	No	1	12×16	1.74	0.8	Pressure
[31]	ISO14443	No	1	26	1.72	1	Skin moisture and UV light
[32]	ISO14443	No	1	26	NA	1	Skin moisture
[33]	ISO14443	No	NA	35x25	1.8	1	ECG and sweat pH
[34]	ISO14443	No	NA	10×5	0.9	1	Arterial SPO2 and Temp
[35]	ISO15693	No	1	25x25	NA	1.4	Moisture
[13]	ISO15693	No	1	50x50	5.29	1.8	pH
[36]	ISO14443	No	NA	43×58	4.45	1.9	Carbon dioxide
[11]	ISO15693	No	1	50x50	3	2	Soil moisture, RH and Temp
[12]	ISO15693	No	1	50x50	5.29	2	Color
[37]	ISO14443	Yes	NA	45×30	NA	2	Ascorbic acid
[38]	ISO15693	No	1	50x50	8	1.9	Color
[39]	ISO15693	Yes	NA	70x70	NA	3	pH
[40]	ISO15693	Yes	NA	34×46	1.3	3	Blood flow
[41]	ISO15693	No	1	35×35	2.1	3	Water minerals
[42]	ISO15693	Yes	NA	25x35	NA	4	pH
[43]	ISO15693	Yes	NA	26×26	NA	4.3	Strain and Temp
This Work	ISO15693	No	0.524	49×59	0.597	5	Temp and RH

In the second iteration, V_{DD} was reduced to 1.8 V (with V_{CORE} = 1.8 V, MCU clock source = HSI, f_{I2C} = 16 MHz and f_{I2C} = 16 MHz) reducing the DC power consumption to 6.18 mW. Further, design iterations changed the clock source to use a low power multi-speed internal (MSI) RC oscillator, reducing the clock frequency and core voltage as shown in Fig 6. The lowest DC power consumption was achieved at f_{CLK} = 0.524 MHz, f_{I2C} = 1.024 MHz, MCU clock source = MSI, V_{CORE} = 1.2 V, and V_{DD} = 1.8 V. The final optimized NFC sensor has a measured DC power consumption of approximately 597 μW when the smartphone was placed at a distance of approximately 2 cm from the NFC sensor. As shown in Fig. 6, the use of the described frequency and voltage scaling techniques enable a factor of greater than 20 % reduction in DC power consumption for the NFC temperature and humidity sensor.

IV. DISCUSSION

This section discusses the performance evaluation and practical deployment of the developed battery-less NFC sensor in a museum.

A. Performance Evaluation

Table II shows a performance comparison of the developed NFC sensor transponder with the current state-of-the-art from relevant literature and highlights the achieved performance improvements compared to the literature. Table II column F shows the overall DC power consumption of battery-less NFC sensor transponders that included a microcontroller as a processing unit exceeds a value of 0.9 mW. In addition, it is evident from Table II (column G) that a wireless communication range of the NFC sensor transponder that included a microcontroller is reported less than 3 cm. It is known [45], [46] that magnetic field strength decays proportionally to the cube of the distance between two mutually-coupled coils [26]. Therefore, in order to reduce overall DC power consumption and increase the communication range, the MCU clock frequency (f_{CLK}) of over half of the NFC sensor transponders reported in Table II was decreased and set to 1 MHz (also referred to as the frequency scaling technique). The overall power consumption also can be reduced by decreasing the CPU core voltage (V_{CORE}) of the MCU (also referred to as a voltage scaling technique) [26]. It is evident from the table that the DC power consumption (0.597 mW) achieved in this work is the lowest reported in the literature. In addition, the wireless communication range (5 cm) of the developed NFC sensor is the largest compared to the state-of-the-art literature. Note that Table II is sorted in increasing order of wireless communication range in column G.

B. Practical Deployment of NFC Sensor in a Museum

This subsection describes the deployment of the developed smart archive box with integrated NFC sensor in Cork Public Museum (CPM), Cork, Ireland. This museum was established in 1910 and houses more than 40 thousand artefacts.

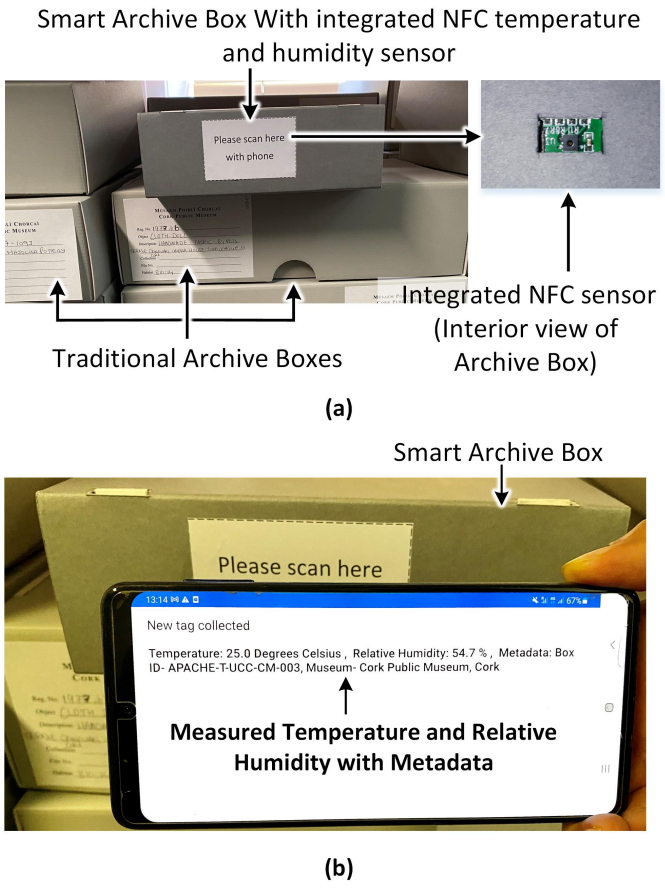


Fig. 7. Deployment at CPM, Ireland (a) smart archive box, (b) measurement

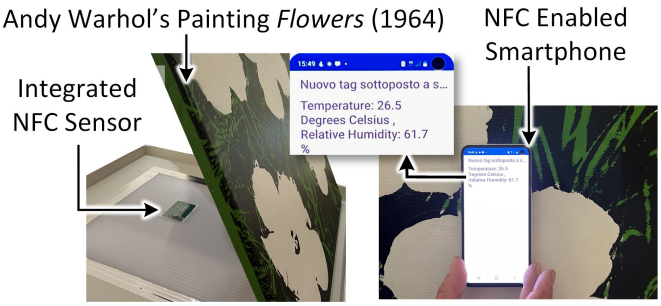


Fig. 8. Deployment of NFC sensor at Guggenheim museum, Venice, Italy.

Fig. 7 (a) shows the deployed smart archive box in the storage facility of the museum. Fig 7 (b) demonstrates the NFC sensor being wirelessly powered and read using a Samsung Galaxy S20 smartphone. When placed within a distance of 5 cm of the sensor, the smartphone enables passive measurement of temperature and relative humidity and additional metadata to be read wirelessly. In addition, the NFC sensor was also deployed at the Guggenheim Museum Venice, Italy to monitor interior temperature and relative humidity of the historic Andy Warhol's "Flowers" which was painted in 1964. Fig 8 shows the NFC sensor integration within the painting frame.

V. Conclusions

This paper presents the performance characterization of a battery-less NFC sensor transponder for museum artifact monitoring. The RF receiver sensitivity of the developed NFC sensor was measured using a commercial Tagformance Pro measurement system. The NFC sensor required a minimum magnetic field strength H_{MIN} of 67.8 mA/m at 13.74 MHz in free space, and 87.6 mA/m at 13.59 MHz when the NFC sensor was integrated within an archive box. In addition, the -3 dB bandwidth of the NFC loop antenna was calculated to be 1.16 MHz and 1.14 MHz respectively for free-space and archive box integration scenarios. The key performance parameters, such as RF receiver sensitivity, centre frequency and bandwidth of the developed NFC sensor were shown to be in close agreement with ISO/IEC 15693 specification. The NFC sensor was also optimized for low power operation using voltage and frequency-scaling techniques for the microcontroller. The power optimization resulted in a peak DC power consumption of 597 μW, which is the lowest value found in the literature. Wireless communications performance tests on the prototype sensor in free space achieved a maximum range of 5 cm with a Samsung Galaxy S20 smartphone and 17.5 cm using the Tagformance pro measurement system. Finally, the developed NFC sensor transponder was successfully deployed in Cork Public Museum, Ireland. In addition, to monitor interior microclimatic condition of the historic Andy Warhol's "Flowers" which was painted in 1964, the NFC sensor was also deployed at the Guggenheim Museum, Venice, Italy.

Acknowledgment

We would like to acknowledge funding support from the European Union's Horizon 2020 and Europe research and innovation program for APACHE project under grant agreement number 814496 and AURORA (Call: HORIZON-CL2-2022-HERITAGE-01, Proposal number: 101094245). Aspects of this work have been supported under the following Grant Numbers: SFI Centre VistaMilk (SFI 16/RC/3835), CONNECT Centre (13/RC/2077), Insight Centre (SFI/12/RC/2289) and 16/RC/3918-CONFIRM, as well as the Enterprise Ireland funded Holistics DTIF (EI-DT20180291-A). All work is co-funded under the European Regional Development Fund.

References

[1] J. Ashley-Smith, A. Burmester, and M. Eibl, *Climate for Collections-Standards and Uncertainties. Postprints of the Munich Climate Conference 7 to 9 November 2012*. Doerner Institut, 2013.

[2] P. Haigh, M. Hayes, D. R. Gawade, and B. O'Flynn, "Towards autonomous smart sensing systems," in *2020 IEEE International Instrumentation and Measurement Technology Conference (I2MTC)*. IEEE, 2020, pp. 1–6.

[3] B. S. Institution, *Specification for Managing Environmental Conditions for Cultural Collections: PAS 198: 2012*. British Standards Limited, 2012.

[4] D. R. Gawade *et al.*, "A battery-less nfc sensor transponder for museum artefact monitoring-a review of nfc sensor technology and a proposed solution," in *SENSORCOMM 2019*. IARIA, 2019.

[5] S. Kumar, J. L. Buckley, J. Barton, M. Pigeon, R. Newberry, M. Rodencal, A. Hajzeraj, T. Hannon, K. Rogers, D. Casey *et al.*, "A wristwatch-based wireless sensor platform for iot health monitoring applications," *Sensors*, vol. 20, no. 6, p. 1675, 2020.

[6] S. Kumar, J. Buckley, J. Barton, and B. O'Flynn, "Performance analysis of a novel flexible nfc tag for iot applications," 2018.

[7] D. R. Gawade, R. B. Simorangkir, D. Zorbas, S. Kumar, S. Ziemann, D. Iacopino, J. Barton, K. Schuhmann, M. Anders, B. O'Flynn *et al.*, "A museum artefact monitoring testbed using lorawan," in *2021 IEEE Symposium on Computers and Communications (ISCC)*. IEEE, 2021, pp. 1–3.

[8] C. Peres *et al.*, "Theoretical models for underwater rfid and the impact of water salinity on the design of wireless systems," *International Journal on Advances in Networks and Services*, vol. 13, no. 34, pp. 45–59, 2020.

[9] M. Boada, A. Lazaro, R. Villarino, E. Gil-Dolcet, and D. Girbau, "Battery-less nfc bicycle tire pressure sensor based on a force-sensing resistor," *IEEE Access*, vol. 9, pp. 103 975–103 987, 2021.

[10] I. Cappelli *et al.*, "Battery-less hf rfid sensor tag for soil moisture measurements," *IEEE Transactions on Instrumentation and Measurement*, vol. 70, pp. 1–13, 2020.

[11] M. Boada, A. Lazaro, R. Villarino, and D. Girbau, "Battery-less soil moisture measurement system based on a nfc device with energy harvesting capability," *IEEE Sensors Journal*, vol. 18, no. 13, pp. 5541–5549, 2018.

[12] A. Lazaro, M. Boada, R. Villarino, and D. Girbau, "Color measurement and analysis of fruit with a battery-less nfc sensor," *Sensors*, vol. 19, no. 7, p. 1741, 2019.

[13] M. Boada, A. Lazaro, R. Villarino, and D. Girbau, "Battery-less nfc sensor for ph monitoring," *IEEE Access*, vol. 7, pp. 33 226–33 239, 2019.

[14] C. Strangfeld, S. Johann, and M. Bartholmai, "Smart rfid sensors embedded in building structures for early damage detection and long-term monitoring," *Sensors*, vol. 19, no. 24, p. 5514, 2019.

[15] P. Escobedo *et al.*, "Flexible passive near field communication tag for multigas sensing," *Analytical chemistry*, vol. 89, no. 3, pp. 1697–1703, 2017.

[16] D. R. Gawade, B. V. B. Roy Simorangkir, S. Kumar, M. Pigeon, M. Belcastro, N. Rather, J. L. Buckley, and B. O'Flynn, "A battery-less nfc sensor transponder for cattle health monitoring," in *2023 IEEE Applied Sensing Conference (APSCON)*, 2023, pp. 1–3.

[17] A. Eldebiky, M. Elsobky, H. Richter, and J. N. Burghartz, "Humidity and temperature sensor system demonstrator with nfc tag for hysif applications," *Advances in Radio Science*, vol. 16, pp. 109–116, 2018.

[18] L. Fiore, V. Mazzaracchio, A. Serani, G. Fabiani, L. Fabiani, G. Volpe, D. Moscone, G. M. Bianco, C. Occhiuzzi, G. Marrocco *et al.*, "Microfluidic paper-based wearable electrochemical biosensor for reliable cortisol detection in sweat," *Sensors and Actuators B: Chemical*, vol. 379, p. 133258, 2023.

[19] F. Nikbakhtnasrabadi, E. S. Hosseini, S. Dervin, D. Shakthivel, and R. Dahiya, "Smart bandage with inductor-capacitor resonant tank based printed wireless pressure sensor on electrospun poly-l-lactide nanofibers," *Advanced Electronic Materials*, vol. 8, no. 7, p. 2101348, 2022.

[20] R. Zhao, P. Wang, Y. Ma, P. Zhang, H. H. Liu, X. Lin, X. Zhang, C. Xu, and M. Zhang, "Nfc+ breaking nfc networking limits through resonance engineering," in *Proceedings of the Annual conference of the ACM Special Interest Group on Data Communication on the applications, technologies, architectures, and protocols for computer communication*, 2020, pp. 694–707.

[21] B. Saggin, J. Podlecki, A. Vena, B. Sorli, F. Coffigniez, V. Guillard, S. Silvestre, and C. Ramade, "Food spoilage estimation using a sensing rfid tag," in *2022 3rd URSI Atlantic and Asia Pacific Radio Science Meeting (AT-AP-RASC)*. IEEE, 2022, pp. 1–4.

[22] S. Nappi, C. Miozzi, V. Mazzaracchio, L. Fiore, F. Camera, N. D'Uva, S. Amendola, C. Occhiuzzi, F. Arduini, and G. Marrocco, "A plug&play flexible skin sensor for the wireless monitoring of pandemics," in *2021 IEEE International Conference on Flexible and Printable Sensors and Systems (FLEPS)*. IEEE, 2021, pp. 1–4.

[23] D. R. Gawade, "Development of a low-power, battery-less near field communication sensor transponder for wireless sensing applications," *CORA, University College Cork*, 2022.

[24] *Tagformance Pro Measurement System Manual*, (accessed March 2023). [Online]. Available: https://voyantic.com/lab/tagformance-pro/ 2020

[25] *Tagformance Pro Measurement System Manual*, (accessed Sept. 2022). [Online]. Available: https://voyantic.com/lab/tagformance-pro/.

[26] D. R. Gawade, S. Ziemann, S. Kumar, D. Iacopino, M. Belcastro, D. Alfieri, K. Schuhmann, M. Anders, M. Pigeon, J. Barton *et al.*, "A smart archive box for museum artifact monitoring using battery-less temperature and humidity sensing," *Sensors*, vol. 21, no. 14, p. 4903, 2021.

[27] K. Paul, D. R. Gawade, R. B. Simorangkir, B. O'Flynn, J. L. Buckley, A. Amann, and S. Roy, "A concertina-shaped vibration energy harvester-assisted nfc sensor with improved wireless communication range," *IEEE Internet of Things Journal*, vol. 9, no. 24, pp. 25 474–25 486, 2022.

[28] *Cards and security devices for personal identification — Contactless vicinity objects —Part 2: Air interface and initialization — Part 2*, (accessed March 2023). [Online]. Available: https://www.iso.org/standard/73601.html.

[29] T. H. Lee, *The design of CMOS radio-frequency integrated circuits*. Cambridge university press, 2003.

[30] Lazaro *et al.*, "Study on the reading of energy-harvested implanted nfc tags using mobile phones," *IEEE Access*, vol. 8, pp. 2200–2221, 2020.

[31] S. M. Ali, T.-B. Nguyen, and W.-Y. Chung, "New directions for skincare monitoring: An nfc-based battery-free approach combined with deep learning techniques," *IEEE Access*, vol. 10, pp. 27 368–27 380, 2022.

[32] S. M. Ali and W.-Y. Chung, "Monitoring transepidermal water loss and skin wettedness factor with battery-free nfc sensor," *Sensors*, vol. 20, no. 19, p. 5549, 2020.

[33] B. M. G. Rosa, S. Anastasova-Ivanova, and G. Z. Yang, "Nfc-powered flexible chest patch for fast assessment of cardiac, hemodynamic, and endocrine parameters," *IEEE Transactions on Biomedical Circuits and Systems*, vol. 13, no. 6, pp. 1603–1614, 2019.

[34] B. M. Rosa, S. Anastasova, and G. Z. Yang, "Nfc-powered implantable device for on-body parameters monitoring with secure data exchange link to a medical blockchain type of network," *IEEE Transactions on Cybernetics*, 2021.

[35] A. Lazaro, M. Boada, R. Villarino, and D. Girbau, "Battery-less smart diaper based on nfc technology," *IEEE Sensors Journal*, vol. 19, no. 22, pp. 10 848–10 858, 2019.

[36] P. Escobedo Araque, M. D. Fernández Ramos, N. López Ruiz, Ó. Moyano-Rodríguez, A. Martínez Olmos, I. M. Pérez de Vargas Sansalvador, M. Á. Carvajal Rodríguez, L. F. Capitán Vallvey, A. J. Palma López *et al.*, "Smart facemask for wireless co2 monitoring," 2022.

[37] K. Krorakai, S. Klangphukhiew, S. Kulchat, and R. Patramanon, "Smartphone-based nfc potentiostat for wireless electrochemical sensing," *Applied Sciences*, vol. 11, no. 1, p. 392, 2021.

[38] M. Boada, A. Lazaro, R. Villarino, and D. Girbau, "Nfc battery-less colour sensor and its applications," in *2020 Global Congress on Electrical Engineering (GC-ElecEng)*. IEEE, 2020, pp. 46–50.

[39] W. Dang, L. Manjakkal, W. T. Navaraj, L. Lorenzelli, V. Vinciguerra, and R. Dahiya, "Stretchable wireless system for sweat ph monitoring," *Biosensors and Bioelectronics*, vol. 107, pp. 192–202, 2018.

[40] B. Vennemann, D. Obrist, and T. Rösgen, "A smartphone-enabled wireless and batteryless implantable blood flow sensor for remote monitoring of prosthetic heart valve function," *PLoS One*, vol. 15, no. 1, p. e0227372, 2020.

[41] X. Qian, Z. Li, Z. Meng, N. Gao, and Z. Zhang, "Flexible rfid tag for sensing the total minerals in drinking water via smartphone tapping," *IEEE Sensors Journal*, vol. 21, no. 21, pp. 24 749–24 758, 2021.

[42] R. Rahimi, U. Brener, S. Chittiboyina, T. Soleimani, D. A. Detwiler, S. A. Lelievre, and B. Ziaie, "Laser-enabled fabrication of flexible and transparent ph sensor with near-field communication for in-situ monitoring of wound infection," *Sensors and Actuators B: Chemical*, vol. 267, pp. 198–207, 2018.

[43] P. Escobedo, M. Bhattacharjee, F. Nikbakhtnasrabadi, and R. Dahiya, "Smart bandage with wireless strain and temperature sensors and batteryless nfc tag," *IEEE Internet of Things Journal*, vol. 8, no. 6, pp. 5093–5100, 2020.

[44] G. Paterakis, E. Vaughan, D. R. Gawade, R. Murray, G. Gorgolis, S. Matsalis, G. Anagnostopoulos, J. L. Buckley, B. O'Flynn, A. J. Quinn *et al.*, "Highly sensitive and ultra-responsive humidity sensors based on graphene oxide active layers and high surface area laser-induced graphene electrodes," *Nanomaterials*, vol. 12, no. 15, p. 2684, 2022.

[45] Q. Jun, H. Chao, Y. Yunhan, and Q. Jizui, "Application of modern communication technology in smart home system," in *2018 IEEE International Conference on Information and Automation (ICIA)*. IEEE, 2018, pp. 1577–1581.

[46] E. Freudenthal, D. Herrera, F. Kautz, C. Natividad, A. Ogrey, J. Sipla, A. Sosa, C. Betancourt, and L. Estevez, "Suitability of nfc for medical device communication and power delivery," in *2007 IEEE Dallas Engineering in Medicine and Biology Workshop*. IEEE, 2007, pp. 51–54.